Comparisons of the Symmetric and Asymmetric Control Limits for $\bar{X}$ and R Charts

Huifen Chen
Department of Industrial and Systems Engineering, Chung-Yuan University
200 Chung-Pei Rd., Chung Li, Taiwan
and
Wei-Lun Kuo
Macronix International Company
16 Li-Hsin Road, Science Park, Hsin-Chu, Taiwan

June 11, 2010

Abstract

Though both symmetric and asymmetric control limits can be applied to $\bar{X}$ and R charts, no well-controlled comparison of the resulting performance has been conducted. Symmetric limits such as 3-sigma limits are the customary choice. However, previous researchers have proposed asymmetric control limits as a more appropriate choice than symmetric limits for skewed distributions. This paper examines the relative performance of symmetric and asymmetric limits. It compares the out-of-control ARL (average run length) for symmetric and asymmetric limits for fixed values of the in-control ARL. Two testing examples are employed: the exponential and Johnson unbounded distributions. The results of the performance comparison are mixed. For both $\bar{X}$ and R charts, the impact of the control limit choice (symmetric or asymmetric) depends on two factors: the skewness of the charting statistic (sample mean $\bar{X}$ for the $\bar{X}$ chart and sample range R for the R chart) and the shift direction. When the charting statistic has a right skewed distribution, symmetric limits perform better if the monitored process property (the mean for the $\bar{X}$ chart and the standard deviation for the R chart) shifts upward, but worse when it shifts downward. When the charting statistic has a left skewed distribution, the outcome is reversed. Although neither type of control limits dominates even for a skewed population, the asymmetric limits are more robust to the shift in the process mean or variation. The effect of the sample size is also discussed.

Keywords: Asymmetric control limits, average run length, shift, skewed distribution, SPC

1 Introduction

In this paper, we compare the impact of control limit settings (symmetric versus asymmetric) on the performance of Shewhart control charts. Both $\bar{X}$ and R charts are used in statistical process control (SPC) to monitor the process mean and variance. A conventional choice for both charts is the symmetric control limits $\mu_Y \pm k\sigma_Y$, where μ_Y and σ_Y are the mean and variance of the charting statistic Y (the sample mean for the $\bar{X}$ chart and sample range for the R chart) and k is a positive constant, typically $k = 3$ (Montgomery, 2005).

Various methods of computing asymmetric control limits for skewed distributions have been proposed.[1] The probability-symmetric approach sets the lower control limit (LCL) and upper control limit (UCL) so that the charting statistic Y is equally likely to fall above the UCL or below the LCL when the process is in-control. That is, when the process is in control, $\mathrm{P}\{Y \leq \mathrm{LCL}\} = \mathrm{P}\{Y \geq \mathrm{UCL}\} = \alpha/2$, where α is the desired Type-I risk.[2] The probability-symmetric control limits are symmetric at μ_Y only if the distribution of Y is symmetric.

If the distribution function of the quality measurement X is unknown, the values of the probability-symmetric control limits must be approximated. A number of methods are available. The weighted variance (WV) method was developed by Choobineh and Ballard (1987) based on semivariance approximation (Choobineh and Branting, 1986). Heuristic variants of the WV method that requires no assumptions concerning the functional form of the distribution were later proposed by, e.g., Bai and Choi (1995), Castagliola (2000), and Castagliola and Tsung (2005). The skewness correction (SC) method (Chan and Cui, 2003) works for skewed distributions. Another approach is to fit a theoretical frequency curve, such as a member of the Pearson system, and obtain probability-symmetric control limits meeting the specified Type-I risk α value.

Some SPC approaches have been developed specifically for skewed distributions. The

[1] An alternative is to transform nonnormal into normal quality measurements and use conventional Shewhart chart limits.

[2] Recall that Type-I risk denotes the probability that Y falls outside the control limits when the process is actually in control.

split distribution method of Cowden (1957) works for arbitrary skewed distributions. Other methods are distribution specific, including geometric midrange and range charts for monitoring the mean and variance of lognormal distributions (Ferrell, 1958) and median, range, scale, and location charts for Weibull distributions (Nelson, 1979).

Although the construction of asymmetric control limits for skewed distributions has been addressed in the literature, little is known about how the adoption of asymmetric control limits affects $\bar{X}$ and R chart performance. In particular, the performance impact of limit choice (symmetric or asymmetric) must be characterized in detail using a consistent benchmark. In this work, we compare the performance impact of symmetric and asymmetric limits (probability-symmetric control limits) for a quality measurement X with a known distribution. Our performance benchmark is the average run length (ARL) when the process goes out of control (called out-of-control ARL). Throughout the comparison, the in-control ARL remains fixed, where the in-control ARL is the ARL when the process is in control. That is, the values of the symmetric and asymmetric control limits are chosen to meet a specified value of the in-control ARL (or equivalently the Type-I risk).

The rest of this paper is organized as follows. Section 2 introduces the symmetric and asymmetric control limits for $\bar{X}$ and R charts. Section 3 presents example computation of the symmetric and asymmetric limits given quality measurements from two different distributions: the exponential and Johnson unbounded distributions (Johnson, 1949). Section 4 compares the performance outcome of symmetric and asymmetric limits with $\bar{X}$ and R charts. The ARL value for the exponential population is computed numerically while the ARL for the Johnson population is estimated via simulation experiments. Our results show that the performance impact of the control limits depends on two factors: the skewness of the charting statistic (right versus left) and the shift direction. We find that even when the distribution of the quality characteristic is skewed, symmetric limits sometimes outperform asymmetric limits. Section 5 concludes.

2 Symmetric and Asymmetric Control Limits

Consider a process that produces sequential outputs. Suppose that each output has a measurable quality characteristic. Let $\bar{X}$ and R denote the average and range of the random sample $\{X_1,\ X_2,\cdots,\ X_n\}$, where $X_1,\ X_2,\cdots$ are successive independent observations of

the quality characteristic measurement X. Let μ_0 and σ_0 denote the mean and standard deviation of X when the process remains in control. To make the comparisons of symmetric and asymmetric control limits simple, we assume that when the process goes out of control, the process mean shifts from μ_0 to $\mu_0 + \delta\sigma_0$ (where δ is a real number) and the process standard deviation shifts from σ_0 to $\gamma\sigma_0$ ($\gamma > 0$), but the higher moments remain unchanged. Such assumption is common in literature, e.g., Castagliola (2000) and Chan and Cui (2003), although it may not be valid in practice. Consider the situation that the distribution shape changes but the process mean and standard deviation remain unchanged when the process goes out of control. The charting statistics $\bar{X}$ and R may fall outside control limits and false alarms occur because the process mean and standard deviation are unchanged. Consequently, comparisons of symmetric and asymmetric limits become complicate.

Shewhart $\bar{X}$ and R charts can detect a shift in the process mean and variance. Both charts contain a center line (CL), UCL, and LCL. Random samples of size n are collected and their sample averages and ranges are plotted in the $\bar{X}$ and R charts. As soon as a point falls outside the control limits, an out-of-control-action plan can be activated to identify and eliminate assignable causes.

If conventional symmetric control limits are used, the CL, UCL, and LCL of the $\bar{X}$ chart are

$$\bar{X}\text{-chart symmetric limits:} \begin{cases} \text{UCL}_{\bar{X}} &= \mu_0 + k_{\bar{X}} \frac{\sigma_0}{\sqrt{n}}, \\ \text{CL}_{\bar{X}} &= \mu_0, \\ \text{LCL}_{\bar{X}} &= \mu_0 - k_{\bar{X}} \frac{\sigma_0}{\sqrt{n}}, \end{cases} \tag{1}$$

and the CL, UCL, and LCL of the R chart are

$$R\text{-chart symmetric limits:} \begin{cases} \text{UCL}_R &= \mu_R + k_R\, \sigma_R, \\ \text{CL}_R &= \mu_R, \\ \text{LCL}_R &= \max\{0,\ \mu_R - k_R\, \sigma_R\}, \end{cases} \tag{2}$$

where μ_R and σ_R denote the mean and standard deviation of the range R. The values of the positive constants $k_{\bar{X}}$ and k_R can be chosen to meet the desired value of the in-control ARL, denoted ARL_0, or equivalently the Type-I risk α ($= 1/\text{ARL}_0$).

If asymmetric control limits are used, then when the process is in control the charting statistic ($\bar{X}$ or R) is equally likely to fall below the LCL or above the UCL. Furthermore, if

the control limits are chosen to meet the desired ARL_0 value, the corresponding CL, UCL, and LCL of the $\bar{X}$ chart are

$$\bar{X}\text{-chart asymmetric limits:} \begin{cases} \text{UCL}_{\bar{X}} &= F_{\bar{X}}^{-1}(1-\frac{\alpha}{2}), \\ \text{CL}_{\bar{X}} &= \mu_0, \\ \text{LCL}_{\bar{X}} &= F_{\bar{X}}^{-1}(\frac{\alpha}{2}), \end{cases} \tag{3}$$

and the CL, UCL, and LCL of the R chart are

$$R\text{-chart asymmetric limits:} \begin{cases} \text{UCL}_{R} &= F_{R}^{-1}(1-\frac{\alpha}{2}), \\ \text{CL}_{R} &= \mu_R, \\ \text{LCL}_{R} &= F_{R}^{-1}(\frac{\alpha}{2}), \end{cases} \tag{4}$$

where the Type-I risk $\alpha = 1/\text{ARL}_0$ and $F_{\bar{X}}$ and F_R are the cumulative distribution functions (CDFs) of $\bar{X}$ and R, respectively. When X is symmetrically distributed, the $\bar{X}$-chart symmetric and asymmetric control limits are identical. If the distribution of X is skewed but the sample size n is large, then the central limit theorem dictates that the sample mean $\bar{X}$ is nearly normally distributed, and hence the symmetric and asymmetric control limits are close. However, the R-chart symmetric and asymmetric control limits are different unless R is symmetrically distributed, which could happen when the quality characteristic X has a bounded distribution.

3 Two Testing Examples

In this section, we illustrate the computation of symmetric and asymmetric control limits for $\bar{X}$ and R charts. The control limits are calculated under two assumptions: that the quality measurement follows the exponential and Johnson unbounded distributions, and the control limits are set to achieve a desired in-control ARL of ARL_0. The same assumptions will hold for our empirical comparisons in Section 4. We describe the computation in two testing examples below.

(a) Exponential distributions

Suppose that when the process is in control, the quality characteristic X follows an exponential distribution with lower bound 0 and mean $\mu_0 = \lambda$ ($=\sigma_0$), denoted exponential(λ).

In this special case, the $\bar{X}$ and R chart symmetric and asymmetric control limits can be computed numerically. We describe the computations below.

$\bar{X}$ charts:

If $\{X_1, \cdots, X_n\}$ is an independent sample from the exponential(λ) population, $\sum_{i=1}^{n} X_i$ follows a gamma distribution with shape parameter n and scale parameter λ (i.e., the mean $= n\lambda$), denoted gamma(n, λ). The symmetric control limits for the $\bar{X}$ chart are therefore $\mu_0 \pm k_{\bar{X}}\sigma_0/\sqrt{n}$ with $k_{\bar{X}}$ satisfying the equation

$$\begin{aligned} & \mathrm{P}\{\ \bar{X} \notin \mu_0 \pm k_{\bar{X}}\sigma_0/\sqrt{n} \mid \mathrm{E}(X) = \mu_0, \mathrm{V}(X) = \sigma_0^2\} \\ = \ & \mathrm{P}\{\ \sum_{i=1}^{n} X_i \notin n\mu_0 \pm \sqrt{n}k_{\bar{X}}\sigma_0 \mid \mathrm{E}(X) = \mu_0, \mathrm{V}(X) = \sigma_0^2\} \\ = \ & 1 + G(n\mu_0 - \sqrt{n}k_{\bar{X}}\sigma_0) - G(n\mu_0 + \sqrt{n}k_{\bar{X}}\sigma_0) \\ = \ & 1 + G(n\lambda - k_{\bar{X}}\sqrt{n}\lambda) - G(n\lambda + k_{\bar{X}}\sqrt{n}\lambda) \ = \ \alpha, \end{aligned} \tag{5}$$

where the Type-I risk $\alpha = 1/\mathrm{ARL}_0$ and $G(\cdot)$ is the gamma(n, λ) CDF. (Recall that $\mu_0 = \sigma_0 = \lambda$ for the exponential distribution.) Since the Type-I risk is functionally independent of the scale parameter λ, Equation (5) can be rewritten as

$$1 + \tilde{G}(n - k_{\bar{X}}\sqrt{n}) - \tilde{G}(n + k_{\bar{X}}\sqrt{n}) \ = \ \alpha, \tag{6}$$

where $\tilde{G}(\cdot)$ is the gamma(n, 1) CDF. We can solve Equation (6) for $k_{\bar{X}}$ using a numerical root-finding method such as the bisection search.

Similarly, the asymmetric control limits for the $\bar{X}$ chart in Equation (3) can be computed numerically for the exponential population. The upper and lower control limits are

$$\bar{X}\text{-chart asymmetric limits:} \begin{cases} \mathrm{UCL}_{\bar{X}} &= F_{\bar{X}}^{-1}\left(1 - \frac{\alpha}{2}\right) = n^{-1}G^{-1}\left(1 - \frac{\alpha}{2}\right), \\ \mathrm{LCL}_{\bar{X}} &= F_{\bar{X}}^{-1}\left(\frac{\alpha}{2}\right) = n^{-1}G^{-1}\left(\frac{\alpha}{2}\right), \end{cases}$$

where $G^{-1}(\cdot)$ denote the inverse of $G(\cdot)$. Both the symmetric and asymmetric limits have the same in-control ARL of $\mathrm{ARL}_0 = 1/\alpha$.

R charts:

R-chart computation of the symmetric and asymmetric control limits is similar to $\bar{X}$-

chart computation. Again, let $\{X_1, \cdots, X_n\}$ be an independent sample from the exponential(λ) population. Then the CDF of the range R is

$$\begin{aligned}
F_R(r) &= n\int_0^\infty \frac{1}{\lambda} e^{-\frac{x}{\lambda}} \left[(1-e^{-\frac{x+r}{\lambda}}) - (1-e^{-\frac{x}{\lambda}})\right]^{n-1} dx \\
&= \frac{n}{\lambda}\int_0^\infty e^{-\frac{x}{\lambda}} \left[e^{-\frac{x}{\lambda}} - e^{-\frac{x+r}{\lambda}}\right]^{n-1} dx \\
&= \frac{n}{\lambda}\int_0^\infty e^{-\frac{x}{\lambda}} \sum_{i=0}^{n-1} \mathrm{C}_i^{n-1} (e^{-\frac{x}{\lambda}})^i (-e^{-\frac{x+r}{\lambda}})^{n-1-i} dx \\
&= \frac{n}{\lambda}\sum_{i=0}^{n-1} \mathrm{C}_i^{n-1} \int_0^\infty e^{-\frac{x}{\lambda}} (e^{-\frac{x}{\lambda}})^i (-e^{-\frac{x+r}{\lambda}})^{n-1-i} dx \\
&= \sum_{i=0}^{n-1} \mathrm{C}_i^{n-1} (-e^{-\frac{r}{\lambda}})^{(n-1-i)} \int_0^\infty \frac{n}{\lambda}\, e^{-\frac{nx}{\lambda}} dx \\
&= \sum_{i=0}^{n-1} \mathrm{C}_i^{n-1} (-e^{-\frac{r}{\lambda}})^{(n-1-i)} = \left[1-e^{-r/\lambda}\right]^{n-1}, \quad 0 \le r \le \infty. \qquad (7)
\end{aligned}$$

Hence, the probability density function (PDF) of R is

$$f_R(r) = \frac{\partial F_R(r)}{\partial\, r} = \frac{n-1}{\lambda} e^{-r/\lambda} \left[1-e^{-r/\lambda}\right]^{n-2}, \quad 0 \le r \le \infty.$$

Since the CDF and PDF have closed forms, the mean and variance can be computed analytically. The mean of R is

$$\begin{aligned}
\mu_R &= \int_0^\infty r \frac{n-1}{\lambda} e^{-r/\lambda} \left[1-e^{-r/\lambda}\right]^{n-2} dr = \frac{n-1}{\lambda}\int_0^\infty r e^{-r/\lambda} \left[1-e^{-r/\lambda}\right]^{n-2} dr \\
&= \frac{(n-1)}{\lambda}\int_0^\infty r e^{-r/\lambda} \sum_{i=0}^{n-2} \mathrm{C}_i^{n-2} (-e^{-r/\lambda})^{n-2-i}\, dr \\
&= \frac{(n-1)}{\lambda} \sum_{i=0}^{n-2} \mathrm{C}_i^{n-2} (-1)^{n-2-i} \int_0^\infty r (e^{-r/\lambda})^{n-1-i}\, dr \\
&= \frac{(n-1)}{\lambda} \sum_{i=0}^{n-2} \mathrm{C}_i^{n-2} (-1)^{n-2-i} \left(\frac{\lambda}{n-1-i}\right)^2 = (n-1)\lambda \sum_{i=0}^{n-2} \mathrm{C}_i^{n-2} (-1)^i (i+1)^{-2}\,.
\end{aligned}$$

The variance is $\sigma_R^2 = \mathrm{Var}(R) = \mathrm{E}(R^2) - \mu_R^2$, where

$$\begin{aligned}
\mathrm{E}(R^2) &= \int_0^\infty r^2 \frac{n-1}{\lambda} e^{-r/\lambda} \left[1-e^{-r/\lambda}\right]^{n-2} dr \;=\; \frac{n-1}{\lambda}\int_0^\infty r^2 e^{-r/\lambda} \left[1-e^{-r/\lambda}\right]^{n-2} dr \\
&= \frac{(n-1)}{\lambda}\int_0^\infty r^2 e^{-r/\lambda} \sum_{i=0}^{n-2} \mathrm{C}_i^{n-2} (-e^{-r/\lambda})^{n-2-i}\, dr
\end{aligned}$$

$$
\begin{aligned}
&= \frac{(n-1)}{\lambda} \sum_{i=0}^{n-2} \mathrm{C}_i^{n-2} (-1)^{n-2-i} \int_0^\infty r^2 (e^{-r/\lambda})^{n-1-i}\, dr \\
&= \frac{(n-1)}{\lambda} \sum_{i=0}^{n-2} \mathrm{C}_i^{n-2} (-1)^{n-2-i}\, 2 \left(\frac{\lambda}{n-1-i}\right)^3 \\
&= 2(n-1)\lambda^2 \sum_{i=0}^{n-2} \mathrm{C}_i^{n-2} (-1)^i (1+i)^{-3} \,.
\end{aligned}
$$

The R-chart symmetric control limits are then $\mu_R \pm k_R \sigma_R$, where the positive constant k_R satisfies

$$
\begin{aligned}
&\mathrm{P}\{\ R \notin \mu_R \pm k_R \sigma_R \mid \mathrm{V}(X) = \sigma_0^2\} \\
&= 1 + F_R(\mu_R - k_R\sigma_R) - F_R(\mu_R + k_R\sigma_R) = \alpha, \qquad (8)
\end{aligned}
$$

i.e., the Type-I risk is equal to α and hence, $\mathrm{ARL}_0 = 1/\alpha$. Notice that the Type-I risk, and therefore Equation (8), are functionally independent of λ. To compute the value of k_R, we use a numerical root-finding method such as the bisection search and set $\lambda = 1$ arbitrarily.

Similarly, the asymmetric control limits in Equation (4) for the R chart can be computed analytically using Equation (7) for the exponential distribution. From Equation (7), we obtain the inverse function of F_R as $F_R^{-1}(p) = -\lambda \ln(1 - p^{1/(n-1)})$, $0 \le p \le 1$. Therefore, the upper and lower control limits are

$$
R\text{-chart asymmetric limits:} \begin{cases} \mathrm{UCL}_R &= F_R^{-1}\left(1 - \frac{\alpha}{2}\right) = -\lambda \ln\left[1 - \left(1 - \frac{\alpha}{2}\right)^{1/(n-1)}\right], \\ \mathrm{LCL}_R &= F_R^{-1}\left(\frac{\alpha}{2}\right) = -\lambda \ln\left[1 - \left(\frac{\alpha}{2}\right)^{1/(n-1)}\right] \,. \end{cases} \qquad (9)
$$

(b) Johnson unbounded distributions

The Johnson unbounded distribution (Johnson, 1949) is a transformation of the standard normal distribution. The Johnson and standard normal random variables, which we denote X and Z, are related by the equation $X = \xi + \nu \sinh((Z - \eta_1)/\eta_2)$, $-\infty < X < \infty$, where ξ and ν are location and scale parameters, and η_1 and η_2 are the shape parameters. If $\{X_1, \cdots, X_n\}$ is an independent sample from the Johnson unbounded distribution, then there are no closed form expressions for the distribution functions of the sample mean $\bar{X}$ and sample range R. Therefore, the symmetric and asymmetric control-limits for a specified

Type-I risk α can not be computed analytically. Instead, we apply the simulation approach below, which enables us to derive symmetric and asymmetric $\bar{X}$ and R chart control limits for arbitrary specifications of the ARL_0 value.

$\bar{X}$ charts:

The symmetric control limits for the $\bar{X}$ chart are $\mu_0 \pm k_{\bar{X}}\sigma_0/\sqrt{n}$, where $k_{\bar{X}}$ satisfies the equation $\text{P}\{\bar{X} \notin \mu_0 \pm k_{\bar{X}}\sigma_0/\sqrt{n} | \text{E}(X) = \mu_0, \text{V}(X) = \sigma_0^2\} = \alpha$, where $\alpha = 1/\text{ARL}_0$. Though the value of $k_{\bar{X}}$ is difficult to compute either analytically or numerically for the Johnson unbounded population, it can be estimated through simulation experiments. This is a stochastic root-finding problem, which we solve via the retrospective approximation algorithm by Chen and Schmeiser (2001). Numerical results are given in Section 4.

Since the asymmetric limits for the $\bar{X}$ chart in Equation (3) represent the $[100(\alpha/2)]^{\text{th}}$ and $[100(1-\alpha/2)]^{\text{th}}$ quantiles, we compute them using the quantile estimation algorithm. For any value p in (0, 1), the $100p^{\text{th}}$ quantile $F_{\bar{X}}^{-1}(p)$ can be estimated using b replications as follows:

1. For $i = 1, 2, \cdots, b$:

   Independently generate a sample $\{x_{i1}, \cdots, x_{in}\}$ from the Johnson unbounded distribution and compute the sample mean $\bar{x}_i = \sum_{j=1}^{n} x_{ij}/n$.

2. Rank the $\bar{x}_i$'s from least to greatest, generating the increasing sequence $\bar{x}_{(1)} \leq \bar{x}_{(2)} \leq \cdots \leq \bar{x}_{(b)}$.

3. Compute the sample quantile $\hat{F}_{\bar{X}}^{-1}(p) = (1-a)\bar{x}_{(r)} + a\bar{x}_{(r+1)}$, where $r = \lfloor bp \rfloor$, $a = bp - r$, and $\lfloor \cdot \rfloor$ the "floor" operator, so that $\lfloor bp \rfloor$ is the largest integer that is no greater than bp.

Generating observations of the Johnson unbounded distribution is easy. We first generate a standard-normal random variate z and then transform it into a Johnson unbounded random variate x by using the formula $x = \xi + \nu \sinh((z - \eta_1)/\eta_2)$.

R charts:

Computing the symmetric control limits $\mu_R \pm k_R\sigma_R$ for the R chart is more complicated than for the $\bar{X}$ chart because μ_R and σ_R need to be estimated through simulation. Given μ_R and σ_R, we use the retrospective approximation algorithm to compute a value of k_R

satisfying the equation $\mathrm{P}\{R \notin \mu_R \pm k_R\sigma_R | \mathrm{V}(X) = \sigma_0^2\} = \alpha$, where μ_R and σ_R are computed via simulation procedure as follows.

1. Independently generate h samples from the Johnson unbounded population, each of size n, and find the range for each of the h samples. Repeat this process t times, obtaining ht range observations r_{ij}, $i = 1, \cdots, t$, $j = 1, \cdots, h$.

2. At replication i, calculate the sample average $\bar{r}_i = \sum_{j=1}^{h} r_{ij}/h$ and sample standard deviation $s_i = [\sum_{j=1}^{h}(r_{ij} - \bar{r}_i)^2/(h-1)]^{1/2}$, $i = 1, \cdots, t$.

3. The R-chart mean and standard deviation are then approximated by $\hat{\mu}_R = \bar{\bar{r}} = \sum_{i=1}^{t} \bar{r}_i/t$ and $\hat{\sigma}_R = [\sum_{i=1}^{t}\sum_{j=1}^{h}(r_{ij} - \bar{\bar{r}})^2/(ht-1)]^{1/2}$. The corresponding standard errors are estimated by $se(\hat{\mu}_R) = [\sum_{i=1}^{t}(\bar{r}_i - \bar{\bar{r}})^2/(t(t-1))]^{1/2}$ and $se(\hat{\sigma}_R) = [\sum_{i=1}^{t}(s_i - \hat{\sigma}_R)^2/(t(t-1))]^{1/2}$.

Table 1 gives estimates $\hat{\mu}_R$, $\hat{\sigma}_R$, and the corresponding standard-error estimates (given in parentheses) for the Johnson unbounded distributions with $\mu_0 = 0$, $\sigma_0 = 1$, skewness and kurtosis $(\alpha_3, \alpha_4) = (2, 11)$, (2,70), (5, 70), and sample size $n = 2$, 5.[3] These estimated values of μ_R and σ_R are used in our empirical comparisons in Section 4.

The R-chart asymmetric control limits are computed in a manner similar to the $\bar{X}$ chart asymmetric control limits. The LCL and UCL are taken to be the $[100(\alpha/2)]^{\text{th}}$ and $[100(1-\alpha/2)]^{\text{th}}$ quantiles of the random range R, and hence can be computed using quantile estimation. R-chart quantile estimation is identical to $\bar{X}$-chart quantile estimation, except that for each sample, the sample range is computed rather than the sample mean.

To apply the control limit formulae in Section 3, the user must specify the ARL_0 value. To ensure a consistent benchmark, in our performance comparisons in Section 4 below we will maintain the $\bar{X}$-chart and R-chart ARL_0 at a uniform level.

4 EMPIRICAL COMPARISONS

In this section, we examine how control limit choice (symmetric or asymmetric) affects $\bar{X}$ and R chart performance. The performance measure (the out-of-control ARL, denoted ARL_1) is computed for a fixed value of ARL_0 (the in-control ARL). In each comparison,

[3] Note that $\alpha_3 = \mathrm{E}[(\frac{X-\mu_0}{\sigma_0})^3]$ and $\alpha_4 = \mathrm{E}[(\frac{X-\mu_0}{\sigma_0})^4]$.

for the given chart type ($\bar{X}$ and R chart), both symmetric and asymmetric control limits are computed for the specified ARL_0 value using the methods described in Section 3. Then the corresponding ARL_1 values are calculated for a given value of the mean shift (for the $\bar{X}$ chart) or standard-deviation shift (for the R chart). In our comparisons, a lower value of ARL_1 signifies better performance.

Two simulation experiments are conducted to assess the performance impact of control limit choice (symmetric or asymmetric limits), the first for $\bar{X}$ charts and the second for R charts. In the first experiment, we assume that the process mean shifts from μ_0 to $\mu_0 + \delta\sigma_0$, $\delta \in R$, but the process standard deviation and higher moments remain unchanged. In the second experiment, we assume that the process standard deviation shifts from σ_0 to $\gamma\sigma_0$, $\gamma > 0$, but the process mean and the third and higher moments remain unchanged. Specifically, if Y and X respectively denote the quality measurements when the process is in control and out of control, $X = Y + \delta\sigma_0$ when the process mean shifts and $X = \gamma Y + (1-\gamma)\mu_0$ when the process standard deviation shifts.

In each experiment, the two testing examples discussed in Section 3 are used. We examine the right skewed exponential distribution and the right and left skewed Johnson unbounded distributions.[4] In each experiment, the symmetric and asymmetric control limits employed satisfy $\text{ARL}_0 = 370$, i.e., $\alpha = 1/\text{ARL}_0 = 0.0027$.

The performance measure ARL_1 is the inverse of the power $(1-\beta)$, where β is the Type-II risk. For the $\bar{X}$ chart, we have $\beta = \text{P}\{\bar{X} \in (\text{LCL}_{\bar{X}}, \text{UCL}_{\bar{X}}) | \text{E}(X) = \mu_0 + \delta\sigma_0, \text{V}(X) = \sigma_0^2\}$ and for the R chart, we have $\beta = \text{P}\{R \in (\text{LCL}_R, \text{UCL}_R) | \text{V}(X) = (\gamma\sigma_0)^2\}$, where $(\text{LCL}_{\bar{X}}, \text{UCL}_{\bar{X}})$ and $(\text{LCL}_R, \text{UCL}_R)$ denote the control limits for the $\bar{X}$ and R charts. Computation of the Type-II risk β is analogous to that of the Type-I risk α. (See Section 3.) For the exponential population, α and β are computed numerically; for the Johnson unbounded distribution, they are estimated through simulation. We describe the computation of β for symmetric limits for the exponential distribution below. The computation of β for asymmetric limits is analogous.

For the exponential distribution, the $\bar{X}$-chart $\text{ARL}_1 = 1/(1-\beta)$, where the Type-II risk $\beta = \text{P}\{\bar{X} \in \lambda \pm k_{\bar{X}}\lambda/\sqrt{n} \mid \text{E}(X) = \lambda + \delta\lambda, \text{V}(X) = \lambda^2\}$ and $k_{\bar{X}}$ satisfies Equation (6) with

[4]The family of Johnson unbounded distributions contains symmetric, left skewed, and right skewed distributions. However, because the focus of this paper is skewed distributions, we consider only asymmetric Johnson distributions.

$\text{ARL}_0 = 370$, i.e., $\alpha = 0.0027$. By defining $Y_i = X_i - \delta\lambda$, $i = 1, \cdots, n$, we have

$$\begin{aligned}
\beta &= \text{P}\{\bar{Y} + \delta\lambda \in \lambda \pm k_{\bar{X}}\lambda/\sqrt{n} \mid \text{E}(Y) = \lambda, \text{V}(Y) = \lambda^2\} \\
&= G(n\lambda + k_{\bar{X}}\sqrt{n}\lambda - n\delta\lambda) - G(n\lambda - k_{\bar{X}}\sqrt{n}\lambda - n\delta\lambda) \\
&= \tilde{G}(n + k_{\bar{X}}\sqrt{n} - n\delta) - \tilde{G}(n - k_{\bar{X}}\sqrt{n} - n\delta). \qquad (10)
\end{aligned}$$

Similarly, the R-chart $\text{ARL}_1 = 1/(1-\beta)$, where the Type-II risk $\beta = \text{P}\{R \in \mu_R \pm k_R\sigma_R \mid \text{V}(X) = (\gamma\lambda)^2\}$, μ_R and σ_R are defined in Section 3, and k_R satisfies Equation (8) with $\text{ARL}_0 = 370$, i.e., $\alpha = 0.0027$. By defining $T_i = [X_i - (1-\gamma)\lambda]/\gamma$, $i = 1, \cdots, n$, and R_T the range of $\{T_1, \cdots, T_n\}$, we have

$$\beta = \text{P}\{\gamma\ R_T \in\ \mu_R \pm k_R\sigma_R | \text{V}(T) = \lambda^2\} = F_R\Big(\frac{\mu_R + k_R\sigma_R}{\gamma}\Big) - F_R\Big(\frac{\mu_R - k_R\sigma_R}{\gamma}\Big).$$

First, consider the $\bar{X}$-chart simulation experiment. The parameter values are set as follows: the sample size $n \in \{2, 5\}$, mean shift $\delta \in \{0, \pm.5, \pm1, \pm2\}$, and the Johnson unbounded distribution skewness and kurtosis $(\alpha_3, \alpha_4) \in \{(2, 11), (-2, 11), (5, 70), (-5, 70)\}$.[5] Table 2 presents the simulation results for the exponential distribution and Table 3 for the Johnson unbounded distribution.

In Table 2, column 1 lists the mean shift δ; columns 2 and 3, the ARL_1 value for the symmetric (denoted Sym.) and asymmetric (Asym.) limits of the $\bar{X}$ chart for $n = 2$; and columns 4 and 5, the ARL_1 value for the symmetric and asymmetric limits for $n = 5$. For the right-skewed exponential population, Table 2 shows that when the mean shift is positive (i.e., the mean increases), the symmetric control limits perform better than the asymmetric limits (i.e., ARL_1 is lower); otherwise, they perform worse.

Figure 1 shows the operating characteristic (OC) curve for the exponential distribution with $n = 2$ (Figure 1a) and 5 (Figure 1b). Each graph depicts the relationship between the shift (the horizontal axis) and the probability that $\bar{X}$ falls within the control limits (the vertical axis). This probability is given by $1 - \alpha$ when δ is zero and β, otherwise. The solid line represents the OC curve for the symmetric control limits; the dotted line, the OC curve for the asymmetric limits. Figure 1 contains similar but more information as in Table 2.

[5]Since ARL_0 and ARL_1 are functionally independent of μ_0 and σ_0, the values of μ_0 and σ_0 can be set arbitrarily.

Figure 1 shows that for a positive shift δ, the symmetric control limits have a lower Type-II risk β. On the other hand, for a negative shift δ, the situation is reversed: the asymmetric control limits have a lower Type-II risk β. Notice that when δ decreases from 0, the Type-II risk for the symmetric limits increases to near 1 and then decreases. For those negative δ values with Type-II risk close to 1, the corresponding ARL_1 is large, e.g., $\delta = -1, -2$ for $n = 2$ and $\delta = -0.5$ for $n = 5$ in Table 2.

FIGURE 1

Figure 1 also shows that when the sample size n increases from 2 to 5, the OC curves for the symmetric and asymmetric limits come closer. This is due to the effect of the central limit theorem. The skewness and kurtosis of $\bar{X}$ are

$$\alpha_3(\bar{X}) = \frac{\alpha_3}{\sqrt{n}}, \qquad \alpha_4(\bar{X}) = \frac{\alpha_4 - 3}{n} + 3. \tag{11}$$

As n goes to infinity, $\alpha_3(\bar{X})$ approaches 0 and $\alpha_4(\bar{X})$ approaches 3. Hence, $\bar{X}$ has an asymptotically normal distribution, and both the symmetric and asymmetric limits converge to the symmetric control limits for the normal distribution. Consequently, when n is large, the OC curves for symmetric and asymmetric limits are almost identical.

Table 3 shows the ARL_1 values of the $\bar{X}$ chart for the Johnson unbounded distribution. Here, column 1 lists the Johnson population skewness α_3 and kurtosis α_4; column 2, the mean shift δ; columns 3 and 4, the ARL_1 estimates (denoted $\widehat{\mathrm{ARL}}_1(\bar{X})$) for the symmetric and asymmetric limits with $n = 2$; and columns 5 and 6, the ARL_1 estimates for the symmetric and asymmetric limits with $n = 5$. The standard-error estimates of $\widehat{\mathrm{ARL}}_1(\bar{X})$ are given in parentheses.

Table 3 shows that the performance impact of symmetric and asymmetric control limits depends on the skewness α_3 and mean shift δ. When $\alpha_3 > 0$ (equivalently, $\alpha_3(\bar{X}) > 0$), the symmetric limits perform better than the asymmetric limits if the shift $\delta > 0$ and worse otherwise. Analogously, when $\alpha_3 < 0$, the asymmetric limits perform better if $\delta > 0$ and worse otherwise. Table 3 also shows that the ARL_1 values for $\alpha_3 > 0$ are the same as those for $-\alpha_3$ with the same kurtosis but δ changing sign. For example, for kurtosis 11, the ARL_1 value for $\alpha_3 = 2$ and $\delta = -2$ equals that for $\alpha_3 = -2$ and $\delta = 2$. Furthermore, as the sample

size n increases, the ARL_1 values for the symmetric and asymmetric limits are more alike due to the central limit theorem.

Figure 2 shows "before" and "after" relationships between the process mean and the control limits for the Johnson unbounded distribution with in-control mean $\mu_0 = 0$, standard deviation $\sigma_0 = 1$, skewness and kurtosis (α_3, α_4)=(2,11), $n = 2$, $\text{ARL}_0 = 370$, and δ =2. Figure 2(a) shows the density plot for $\bar{X}$ when the process mean is in control and has expected value 0. Figure 2(b) shows the density plot for $\bar{X}$ when the distribution of the process mean shifts to $\mu_0+2\sigma_0= 2$. In each graph, the symmetric limits ± 3.1 and asymmetric limits $(-1.2, 3.6)$ are represented by solid and dotted lines.

FIGURE 2

Figure 2 shows that when the distribution of X is right skewed (i.e., $\alpha_3 > 0$.) and the mean shift $\delta > 0$, symmetric limits result in a lower Type-II risk than asymmetric limits. Let $\beta^{(s)}$ and $\beta^{(a)}$ denote the Type-II risk for the symmetric and asymmetric limits. As shown in Figure 2(b), $\beta^{(a)}$ exceeds $\beta^{(s)}$, with the difference represented by the shaded area. Hence, symmetric limits perform better when α_3 and δ are both of the same sign (either both positive or both negative). Otherwise, asymmetric control limits perform better.

Secondly, consider the simulation experiment for the R chart. The simulation results for the exponential and Johnson distributions are shown in Tables 4 and 5. Table 4 shows the ARL_1 values for the R-chart symmetric and asymmetric control limits, where the quality characteristic follows an exponential distribution. (Notice that the range R has a positive skewness because the exponential distribution is unbounded on the right and hence, the support of R is $[0, \infty)$.) The parameter values are set as follows: the sample size $n \in \{2, 5, 10\}$, the standard-deviation shift $\gamma \in \{0.5, 0.75, 1, 1.5, 2, 3\}$, and $\text{ARL}_0 = 370$. It yields 18 experimental points. In Table 4, column 1 lists the standard-deviation shift γ, columns 2 and 3 the ARL_1 for the symmetric and asymmetric limits for $n = 2$; columns 4 and 5 the ARL_1 for $n = 5$; columns 6 and 7 the ARL_1 for $n = 10$. Table 4 shows that the symmetric control limits perform better than the asymmetric limits when $\gamma > 1$ and worse when $\gamma < 1$. Moreover, when γ goes to 0, the ARL_1 for the symmetric limits goes to infinity for $n = 2$, 5, 10. This is because in this experiment, the symmetric limits have LCL=0 and hence are less powerful in detecting a downward shift in the standard deviation.

Figure 3 illustrates the symmetric and asymmetric R-chart control limits for the exponential distribution. The exponential in-control mean $\mu_0 = 1$ and in-control standard deviation $\sigma_0 = 1$. Other parameter values are set as follows: the sample size $n = 5$, standard-deviation shift $\gamma = 2$, and $\text{ARL}_0 = 370$. Figures 3(a) and 3(b) respectively show the PDF curve of the range R when the process is in control with standard deviation 1 and out of control with the standard deviation shifts from 1 to 2 (i.e., γ =2). In each graph, the symmetric limits (0, 7.30) and asymmetric limits (0.21, 7.99) are represented by solid and dotted lines.

FIGURE 3

Figure 3 shows that when the distribution of the range R is right skewed and the process standard deviation shifts upward (i.e., $\gamma > 1$), the symmetric control limits provide a lower Type-II risk than the asymmetric limits. Let $\beta_R^{(s)}$ and $\beta_R^{(a)}$ denote the Type-II risk for the symmetric and asymmetric limits. Figure 3(b) shows that $\beta_R^{(a)}$ is larger than $\beta_R^{(s)}$, with difference shown in the shaded area. Hence, the symmetric limits are better than the asymmetric control limits in this case.

Finally we compare the symmetric and asymmetric control limits for the Johnson unbounded distribution. Suppose that the quality characteristic follows a Johnson unbounded distribution with the in-control mean $\mu_0 = 0$ and standard deviation $\sigma_0 = 1$. The parameter values are set as follows: the Johnson unbounded skewness and kurtosis $(\alpha_3, \alpha_4) \in \{(2, 11), (2, 70), (5, 70)\}$, sample size $n \in \{2, 5\}$, shift $\gamma \in \{0.5, 0.75, 1, 1.5, 2, 3\}$, and $\text{ARL}_0 = 370$. It yields 36 experimental points. Only positive values of α_3 are considered since the range R for a Johnson population with skewness α_3 and that for a Johnson with skewness $-\alpha_3$ (and same kurtosis) have the same distribution. The values of symmetric and asymmetric control limits and corresponding ARL_1 are estimated by simulation experiments, using the estimates of μ_R and σ_R that are listed in Table 1.

Table 5 shows the simulation results for the Johnson unbounded distribution. Here, column 1 lists the Johnson skewness α_3 and kurtosis α_4; column 2, the standard-deviation shift γ, column 3, the skewness $\alpha_{3,R}$ of the range R for $n = 2$, columns 4 and 5, the ARL_1 estimates (denoted $\widehat{\text{ARL}}_1(R)$) for the R-chart symmetric and asymmetric limits with $n = 2$; columns 6 to 8, $\alpha_{3,R}$ and $\widehat{\text{ARL}}_1(R)$ for the symmetric and asymmetric limits with $n = 5$.

The standard-error estimates of $\widehat{\mathrm{ARL}}_1(R)$ are given in parentheses. Table 5 shows that the symmetric control limits perform better (i.e., more powerful in detecting an increase in the process variation) than the asymmetric limits when $\gamma > 1$ and worse when $\gamma < 1$. These results coincide with those in Table 4 because the $\alpha_{3,R}$ values in Table 5 are all positive. Despite lack of results for negative $\alpha_{3,R}$ here, our earlier work (Chen and Kuo, 2007) shows that the results for negative $\alpha_{3,R}$ are reversed of those for positive $\alpha_{3,R}$.

5 CONCLUSIONS

This work compares the performance of symmetric and asymmetric control limits for $\bar{X}$ and R charts. The performance measure is the out-of-control ARL, while keeping the in-control ARL at a specified value. Our results show that for both $\bar{X}$ and R charts, the performance of the symmetric and asymmetric limits depend on the skewness of the charting statistic ($\bar{X}$ for the $\bar{X}$ chart and R for the R chart) and the shift direction. If the charting statistic has a right-skewed distribution, the symmetric limits perform better when the monitored process property (mean for the $\bar{X}$ chart and standard deviation for the R chart) shifts upward and worse otherwise. If the charting statistic has a left-skewed distribution, the outcome is reversed. Although neither type of the control limits dominates, the asymmetric limits are more robust to the shift in the process mean or variation.

The skewnesses of the sample mean $\bar{X}$ and sample range R depend on the distribution of the quality characteristic X. Since the skewness of $\bar{X}$ equals the skewness of X divided by $\sqrt{n}$, $\bar{X}$ and X have the same direction of skew. The direction of skew for the range R, however, depends on whether the distribution of X is bounded or unbounded. If the distribution of X is unbounded on one or both sides, R has a right-skewed distribution. If the distribution of X is bounded, the distribution of R is right skewed when the sample size n is small, symmetric when n is moderate, and left skewed when n is large.

The sample size n has different effects on the $\bar{X}$ and R charts. For the $\bar{X}$ chart, the performances of the symmetric and asymmetric limits differ less when the sample size n increases due to the central limit theorem. For the R chart, the difference of the performances of symmetric and asymmetric limits decreases with n when $\gamma > 1$ but increases with n when $\gamma < 1$.

Directions of future research include (1) deriving the asymmetric limits for autocorre-

lated data with nonnormal marginal distribution and (2) comparing the symmetric and asymmetric limits of the $\bar{X}$ and R charts for autocorrelated data.

Acknowledgments

This research is supported by the National Science Council in Taiwan under grant NSC 97-2221-E-033-035.

REFERENCES

Bai, D. S., Choi, I. S. (1995). $\bar{X}$ and R Control Charts for Skewed Populations. *Journal of Quality Technology* **27**, 120–131.

Castagliola, P. (2000). $\bar{X}$ Control Chart for Skewed Populations Using a Scaled Weighted Variance Method. *International Journal of Reliability, Quality and Safety Engineering* **7**, 237–252.

Castagliola, P., Tsung, F. (2005). Autocorrelated SPC for Non-Normal Situations. *Quality and Reliability Engineering International* **21**, 131–161.

Chan, L. K., Cui, H. J. (2003). Skewness Correction $\bar{X}$ and R Charts for Skewed Distributions. *Naval Research Logistic* **50**, 555–573.

Chen, H., Kuo, W. (2007). Comparisons of the Symmetric and Asymmetric Control Limits for R Charts. In *Proceedings of the 8th Asia Pacific Industrial Engineering & Management System (APIEMS) and 2007 Chinese Institute of Industrial Engineers (CIIE) Conference*, Taiwan, December 2007.

Chen, H., Schmeiser, B. W. (2001). Stochastic Root Finding via Retrospective Approximation. *IIE Transactions* **33**, 259–275.

Choobineh, F., Ballard, J. L. (1987). Control-Limits of QC Charts for Skewed Distributions Using Weighted-Variance. *IEEE Transactions on Reliability* **36**, 473–477.

Choobineh, F., Branting, D. (1986). A Simple Approximation for Semivariance. *European Journal of Operational Research* **27**, 364–370.

Cowden, D. J. (1957). *Statistical Methods in Quality Control.* Englewood Cliffs, NJ: Prentice-Hall.

Ferrell, E. B. (1958). Control Charts for Log-normal Universe. *Industrial Quality Control* **15**, 4–6.

Johnson, N.L. (1949). Systems of Frequency Curves Generated by Methods of Translation.

Biometrika **36**, 149–176.

Montgomery, D.C. (2005). *Introduction to Statistical Quality Control* (5th ed.). New York: Wiley.

Nelson, P. R. (1979). Control Charts for Weibull Processes with Standards Given. *IEEE Transactions on Reliability* **28**, 283–287.

Table 1: Values of $\hat{\mu}_R$, $\hat{\sigma}_R$, and their standard-error estimates (in parentheses) for the Johnson unbounded distributions with $\mu_0 = 0$, $\sigma_0 = 1$, skewness and kurtosis $(\alpha_3,\ \alpha_4) =$ (2, 11), (2,70), (5, 70), and sample size $n = 2,\ 5$

	$n = 2$		$n = 5$	
$(\alpha_3,\ \alpha_4)$	$\hat{\mu}_R$	$\hat{\sigma}_R$	$\hat{\mu}_R$	$\hat{\sigma}_R$
(2, 11)	1.0180 (0.0005)	0.980 (0.001)	2.1283 (0.0007)	1.189 (0.001)
(2, 70)	0.9171 (0.0006)	1.072 (0.003)	1.98 (0.001)	1.490 (0.003)
(5, 70)	0.8464 (0.0007)	1.130 (0.003)	1.809 (0.001)	1.547 (0.003)

Table 2: The ARL_1 values of the symmetric and asymmetric $\bar{X}$-chart control limits for the exponential distribution with sample size $n = 2,\ 5$, shift $\delta = 0,\ \pm 0.5,\ \pm 1,\ \pm 2$, and $\mathrm{ARL}_0 = 370$

	$n = 2$		$n = 5$	
δ	Sym. $\mathrm{ARL}_1(\bar{X})$	Asym. $\mathrm{ARL}_1(\bar{X})$	Sym. $\mathrm{ARL}_1(\bar{X})$	Asym. $\mathrm{ARL}_1(\bar{X})$
-2	14062	1.10	1.28	1.02
-1	2245	1.64	47.5	1.46
-0.5	908	3.52	2404	4.23
0	370	370	370	370
0.5	153	303	64.0	122
1	64.2	126	13.1	23.2
2	12.1	22.8	1.36	1.81

Table 3: Estimates $\widehat{\mathrm{ARL}}_1(\bar{X})$ of ARL_1 for the symmetric and asymmetric $\bar{X}$-chart control limits for the Johnson unbounded distribution with skewness and kurtosis $(\alpha_3, \alpha_4) = (2,11)$, $(-2,11)$, $(5,70)$, $(-5,70)$, sample size $n = 2$, 5, shift $\delta = 0$, ± 0.5, ± 1, ± 2, and $\mathrm{ARL}_0 = 370$ (Note: Standard-error estimates for $\widehat{\mathrm{ARL}}_1(\bar{X})$ are given in parentheses.)

		$n = 2$		$n = 5$	
		Sym.	Asym.	Sym.	Asym.
(α_3, α_4)	δ	$\widehat{\mathrm{ARL}}_1(\bar{X})$	$\widehat{\mathrm{ARL}}_1(\bar{X})$	$\widehat{\mathrm{ARL}}_1(\bar{X})$	$\widehat{\mathrm{ARL}}_1(\bar{X})$
	-2	215 (1)	1.1 (0)	1.3 (0)	1 (0)
	-1	1534 (7)	2.3 (0.01)	56 (0.2)	1.6 (0)
	-0.5	766 (3)	9 (0.04)	1763 (8)	6 (0.02)
(2,11)	0	370 (2)	369 (2)	370 (2)	372 (2)
	0.5	173 (0.8)	348 (1.6)	75 (0.3)	155 (0.7)
	1	78 (0.3)	163 (0.7)	16 (0.06)	31 (0.1)
	2	15 (0.06)	32 (0.1)	1.4 (0)	2 (0.01)
	-2	15 (0.06)	32 (0.1)	1.4 (0)	2 (0.01)
	-1	78 (0.3)	163 (0.7)	16 (0.06)	31 (0.1)
	-0.5	173 (0.8)	348 (1.6)	75 (0.3)	155 (0.7)
$(-2,11)$	0	370 (2)	369 (2)	370 (2)	372 (2)
	0.5	766 (3)	9 (0.04)	1763 (8)	6 (0.02)
	1	1534 (7)	2.3 (0.01)	56 (0.2)	1.6 (0)
	2	215 (1)	1.1 (0)	1.3 (0)	1 (0)
	-2	1473 (7)	1.1 (0)	3.65 (0.01)	1.0 (0)
	-1	769 (3)	1.4 (0)	1582.5 (7)	1.2 (0)
	-0.5	544 (2)	3 (0.01)	800 (4)	3 (0.01)
(5,70)	0	372 (2)	370 (2)	372 (2)	370 (2)
	0.5	249 (1)	508 (2)	155 (1)	338 (2)
	1	159 (0.7)	344 (2)	57 (0.3)	137 (1)
	2	58 (0.3)	146 (0.6)	5 (0.02)	16 (0.1)
	-2	58 (0.3)	146 (0.6)	5 (0.02)	16 (0.1)
	-1	159 (0.7)	344 (2)	57 (0.3)	137 (1)
	-0.5	249 (1)	508 (2)	155 (1)	338 (2)
$(-5,70)$	0	372 (2)	370 (2)	372 (2)	370 (2)
	0.5	544 (2)	3 (0.01)	800 (4)	3 (0.01)
	1	769 (3)	1.4 (0)	1582.5 (7)	1.2 (0)
	2	1473 (7)	1.1 (0)	3.65 (0.01)	1.0 (0)

Table 4: The ARL_1 values of symmetric and asymmetric R-chart control limits for the exponential distribution with sample size $n = 2$, 5, 10, shift $\gamma = 0.5$, 0.75, 1, 1.5, 2, 3, and $\mathrm{ARL}_0 = 370$

	$n = 2$		$n = 5$		$n = 10$	
	Sym.	Asym.	Sym.	Asym.	Sym.	Asym.
γ	$\mathrm{ARL}_1(R)$	$\mathrm{ARL}_1(R)$	$\mathrm{ARL}_1(R)$	$\mathrm{ARL}_1(R)$	$\mathrm{ARL}_1(R)$	$\mathrm{ARL}_1(R)$
0.5	137,205	370	547,586	69.3	1,231,606	17.1
0.75	2,660	513	4,217	262	5,524	130
1	370	370	370	370	370	370
1.5	51.6	76.2	32.8	51.1	25.2	39.7
2	19.3	26.7	10.0	14.0	6.9	9.5
3	7.2	9.0	3.3	4.0	2.2	2.6

Table 5: Estimates $\widehat{\mathrm{ARL}}_1(R)$ of ARL_1 for the symmetric and asymmetric R-chart control limits for the Johnson unbounded distribution with skewness and kurtosis $(\alpha_3, \alpha_4) = (2,11)$, $(2,70)$, $(5,70)$, sample size $n = 2$, 5, shift $\gamma = 0.5$, 0.75, 1, 1.5, 2, 3, and $\mathrm{ARL}_0 = 370$ (Note: The estimate of the standard error of $\widehat{\mathrm{ARL}}_1(R)$ is listed in parentheses.)

		$n = 2$			$n = 5$		
			Sym.	Asym.		Sym.	Asym.
(α_3, α_4)	γ	$\alpha_{3,R}$	$\widehat{\mathrm{ARL}}_1(R)$	$\widehat{\mathrm{ARL}}_1(R)$	$\alpha_{3,R}$	$\widehat{\mathrm{ARL}}_1(R)$	$\widehat{\mathrm{ARL}}_1(R)$
(2,11)	0.5	2.20	253*10^2 (114)	380 (3)	1.85	434*10^2 (196)	53.6 (0.4)
	0.75		1709 (8)	493 (4)		228*10 (10)	233 (1)
	1		370 (2)	372 (2)		374 (2)	372 (2)
	1.5		64.3 (0.3)	97.3 (0.4)		46.0 (0.2)	79.4 (0.3)
	2		23.8 (0.1)	35.2 (0.2)		14.1 (0.1)	23.0 (0.1)
	3		8.27 (0.04)	11.0 (0.1)		4.01 (0.02)	5.59 (0.02)
(2,70)	0.5	3.93	431*10 (19)	342 (2)	5.53	599*10 (27)	56 (0.4)
	0.75		974 (4)	424 (3)		1128 (5)	226 (1)
	1		370 (2)	371 (2)		372 (2)	371 (2)
	1.5		104 (0.5)	179 (1)		86.4 (0.4)	156 (1)
	2		46.1 (0.2)	83.9 (0.4)		33.6 (0.1)	65.9 (0.3)
	3		16.7 (0.1)	28.9 (0.1)		10.38 (0.04)	18.6 (0.1)
(5,70)	0.5	4.31	449*10 (20)	400 (3)	5.03	643*10 (29)	58.7 (0.4)
	0.75		998 (4)	483 (3)		1110 (5)	228 (1)
	1		370 (2)	367 (2)		371 (2)	370 (2)
	1.5		107 (1)	165 (1)		89.7 (0.4)	159 (1)
	2		49.3 (0.2)	78.3 (0.4)		36.6 (0.2)	62.3 (0.3)
	3		19.4 (0.1)	29.1 (0.1)		12.2 (0.1)	19.2 (0.1)

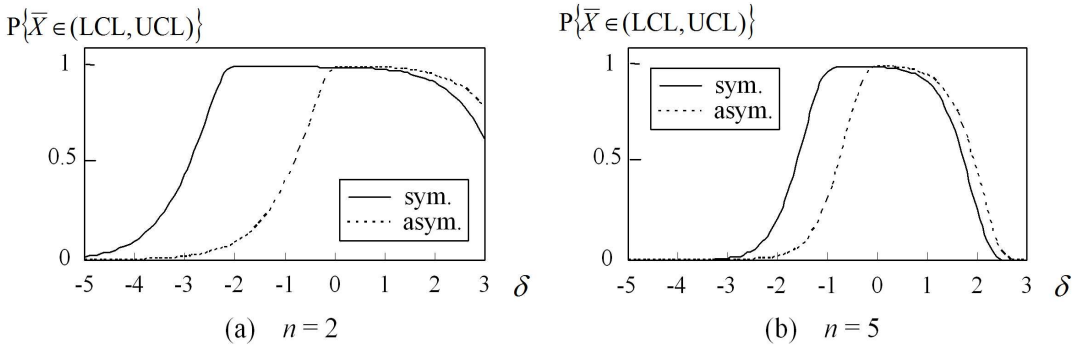

Figure 1: The operating characteristic curves for symmetric and asymmetric control limits and an exponential population with sample size $n = 2$, 5, and $\text{ARL}_0 = 370$

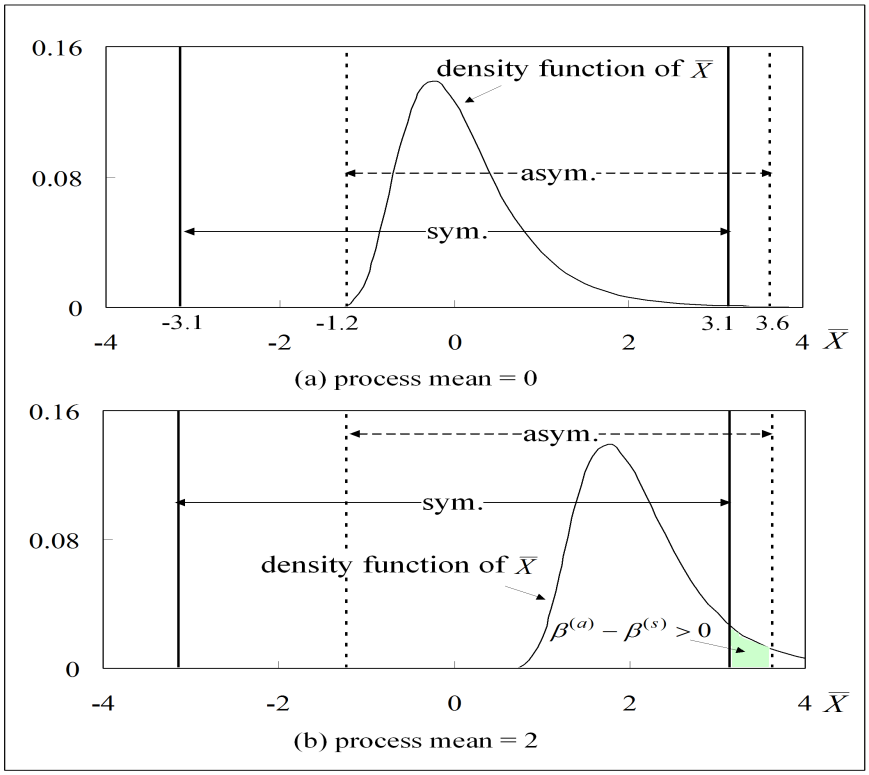

Figure 2: Illustration of the symmetric and asymmetric control limits on the $\bar{X}$ density plot for the Johnson unbounded distribution with the process mean equal to the target $\mu_0 = 0$ in Subfigure (a) and mean shifted to $\mu_0 + 2\sigma_0 = 2$ in Subfigure (b), where the process standard deviation $\sigma_0 = 1$, skewness $\alpha_3 = 2$ and kurtosis $\alpha_4 = 11$ (the skewness and kurtosis of $\bar{X}$ are 1.414 and 7), sample size $n = 2$, and $\text{ARL}_0 = 370$

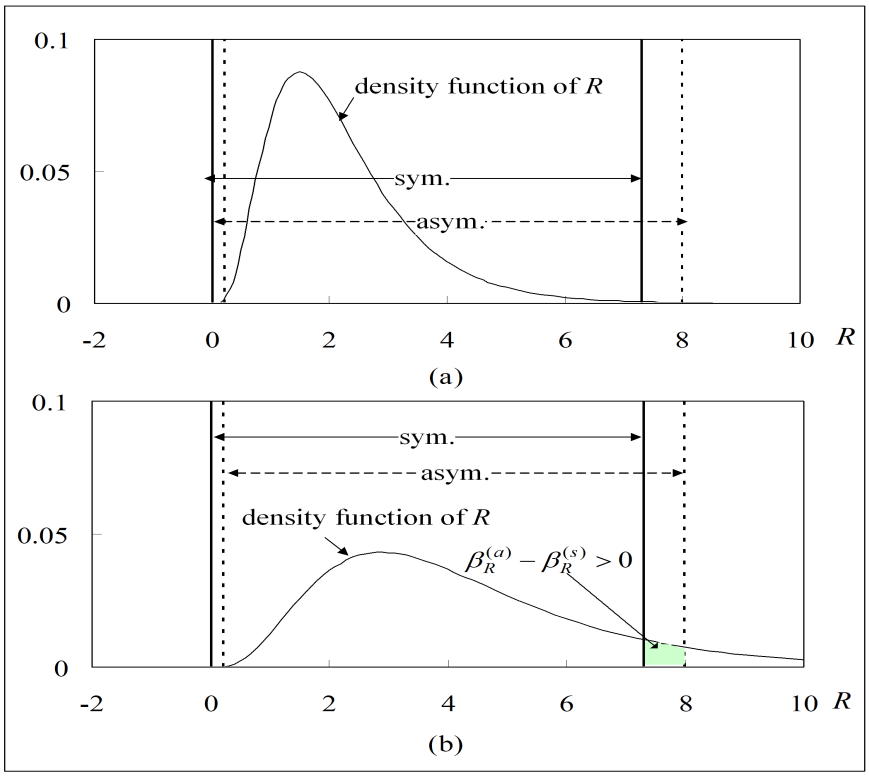

Figure 3: Illustration of the symmetric and asymmetric R-chart limits on the density plot of the range R for the exponential distribution with the standard deviation $\sigma_0 = 1$ (in-control state) in Subfigure (a) and standard deviation shifted to $2\sigma_0 = 2$ (out-of-control state) in Subfigure (b), where the process mean $\mu_0 = 1$, sample size $n = 5$, and $\text{ARL}_0 = 370$